Coherent orbital waves in the photo-induced insulator–metal dynamics of a magnetoresistive manganite

D. POLLI[1]*, M. RINI[2]*, S. WALL[3]*, R. W. SCHOENLEIN[2], Y. TOMIOKA[4], Y. TOKURA[4], G. CERULLO[1] AND A. CAVALLERI[3,5]†

[1]ULTRAS-INFM-CNR Dipartimento di Fisica, Politecnico di Milano, Milano 20133, Italy
[2]Materials Sciences Division, Lawrence Berkeley National Laboratory, Berkeley 94720, USA
[3]Department of Physics, Clarendon Laboratory, University of Oxford, Oxford, OX1 3PU, UK
[4]Correlated Electron Research Center, Tsukuba 305-8562, Japan
[5]Central Laser Facility, Rutherford Laboratory & Diamond Light Source, Chilton, OX11 0DE, UK
*These authors contributed equally to this work
†e-mail: a.cavalleri1@physics.ox.ac.uk

Published online: 12 August 2007; doi:10.1038/nmat1979

Photo-excitation can drive strongly correlated electron insulators into competing conducting phases[1,2], resulting in giant and ultrafast changes of their electronic and magnetic properties. The underlying non-equilibrium dynamics involve many degrees of freedom at once, whereby sufficiently short optical pulses can trigger the corresponding collective modes of the solid along temporally coherent pathways. The characteristic frequencies of these modes range between the few GHz of acoustic vibrations[3] to the tens or even hundreds of THz for purely electronic excitations. Virtually all experiments so far have used 100 fs or longer pulses, detecting only comparatively slow lattice dynamics[4,5]. Here, we use sub-10-fs optical pulses to study the photo-induced insulator–metal transition in the magnetoresistive manganite $Pr_{0.7}Ca_{0.3}MnO_3$. At room temperature, we find that the time-dependent pathway towards the metallic phase is accompanied by coherent 31 THz oscillations of the optical reflectivity, significantly faster than all lattice vibrations. These high-frequency oscillations are suggestive of coherent orbital waves[6,7], crystal-field excitations triggered here by impulsive stimulated Raman scattering. Orbital waves are likely to be initially localized to the small polarons of this room-temperature manganite, coupling to other degrees of freedom at longer times, as photo-domains coalesce into a metallic phase.

$Pr_{(1-x)}Ca_xMnO_3$ is a perovskite manganite with low tolerance factor that maintains semiconducting properties for all temperatures and doping levels[8]. Below 220 K, long-range charge, orbital and magnetic order[9,10] sets in, mediated by a subtle interplay between super-exchange interactions and a long-range Jahn–Teller distortion[11,12]. For $x = 0.3$ doping, the electronically ordered insulator becomes particularly precarious, exhibiting an instability against one or more competing metallic phases and a truly 'colossal' negative magnetoresistance[13]. In addition to the application of a magnetic field, other perturbations can 'melt' the insulating state: photo-excitation[14], application of static electric fields[15], X-ray irradiation[16] and electron irradiation[17]. All of these processes are related to charge injection[18] into the orbitally ordered phase of $Pr_{0.7}Ca_{0.3}MnO_3$.

Ultrafast pulses have indeed been used in the past to manipulate and study the dynamics of photo-induced phase transitions in this[19] and other compounds. However, virtually all experiments so far have been limited to near-100-fs time resolution. This has only revealed dynamics on comparatively slow timescales, and only lattice vibrations at frequencies of a few THz have been detected (~10 meV energy scale). The experiments reported here are carried out with 7 fs pump and 11 fs probe pulses. The order-of-magnitude decrease in pulse duration provides access to coherent modes at frequencies of tens of THz, reaching the hundreds-of-meV energy scale of collective electronic excitations.

We first carried out time-resolved resistivity measurements at 77 K, which substantiate our claim of a photo-induced insulator–metal transition (Fig. 1). A current amplifier was placed in series with the sample, which was held between two gold electrodes deposited on the surface. After femtosecond optical excitation, a prompt resistivity drop was observed from the static value of $3 \times 10^4\ \Omega$ cm to approximately $0.1\ \Omega$ cm, a conductivity change of similar magnitude as that obtained by application of a 6 T magnetic field at this temperature and doping[7]. The photo-induced conductivity exhibits nonlinear growth with fluence above a threshold of $1\ mJ\ cm^{-2}$, saturating above $30\ mJ\ cm^{-2}$. This behaviour and the long lifetime of the high-conductivity state are indicative of cooperativity in the destabilization of charge order and of a photo-induced phase transition.

Figure 2a shows femtosecond pump–probe experiments at 77 K, highlighting the dynamics of the insulator–metal phase change. Optical pulses of 7 fs duration near 550 nm excited the O $2p$-Mn $3d$-e_g charge-transfer resonance in the low-T charge-ordered insulator. The broad bandwidth of the pump pulse coupled the O $2p$ states to a coherent superposition of the Mn-e_g levels. The probe pulse duration was set to 11 fs duration, corresponding to a limited bandwidth and allowing for measurements of the time-dependent reflectivity response in different spectral regions.

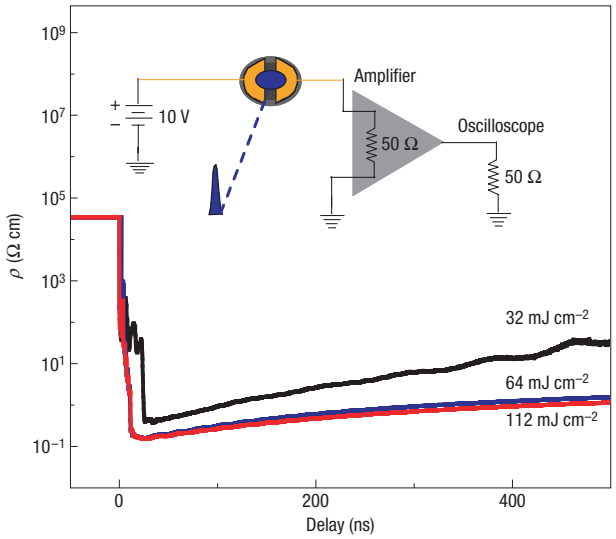

Figure 1 Time-resolved measurement of the nanosecond conductivity transients induced by photo-excitation in single-crystal $Pr_{0.7}Ca_{0.3}MnO_3$ at 77 K. The experimental apparatus is described in the Methods section. The measurements are indicative of a photo-induced change in resistivity of nearly six orders of magnitude.

After photo-excitation, a large reflectivity change was observed. The spectral dependence of the differential reflectivity signal at 500 fs time delay (see Fig. 2a) shows an increase in reflectivity at shorter wavelengths and a decrease at longer wavelengths, reminiscent of the effect seen on application of a magnetic field[20].

The time profile of the differential reflectivity signal, for instance at the 660 nm wavelength shown in Fig. 2a, indicates that the phase transition does not occur promptly[21]. This is clearly indicated by the comparison with the cross-correlation between 7 fs pump and 11 fs probe pulses, measured *in situ*. Two time constants of 50 and 150 fs were found. To further substantiate the delay found in the measured optical response, we measured the time-dependent transmission of a film of C_{60} molecules, which exhibits prompt excited-state absorption and follows the integral of the pump–probe cross-correlation signal.

The delay found in the formation of the product phase is the first important observation of our experiments, which can set a time and thus an energy scale for the ultrafast insulator–metal transition in manganites. The observed bottleneck timescale indicates that the photo-induced metallic state is not driven by sole carrier injection, but requires rearrangement in slower degrees of freedom of the system. Figure 2a also shows the spectral response of the reflectivity at 500 fs time delay, which exhibits a shift of the charge-transfer excitation similar to that observed on application of a magnetic field.

We also found that the reflectivity change is accompanied by coherent modulations with a broad frequency distribution centred at 14 THz (see Fig. 2b). The frequency bandwidth of the oscillations covers many Raman-active modes of perovskite manganites, associated with motions of the oxygen octahedron. This motion is probably coupled both to the static distortion of the cubic perovskite cell (tolerance factor) and to the Jahn–Teller distortion, which stabilize the low-T insulating phase[22]. The near-200-fs damping time of these coherent vibrations can probably be attributed to dephasing of many phonon modes evolving at different frequencies.

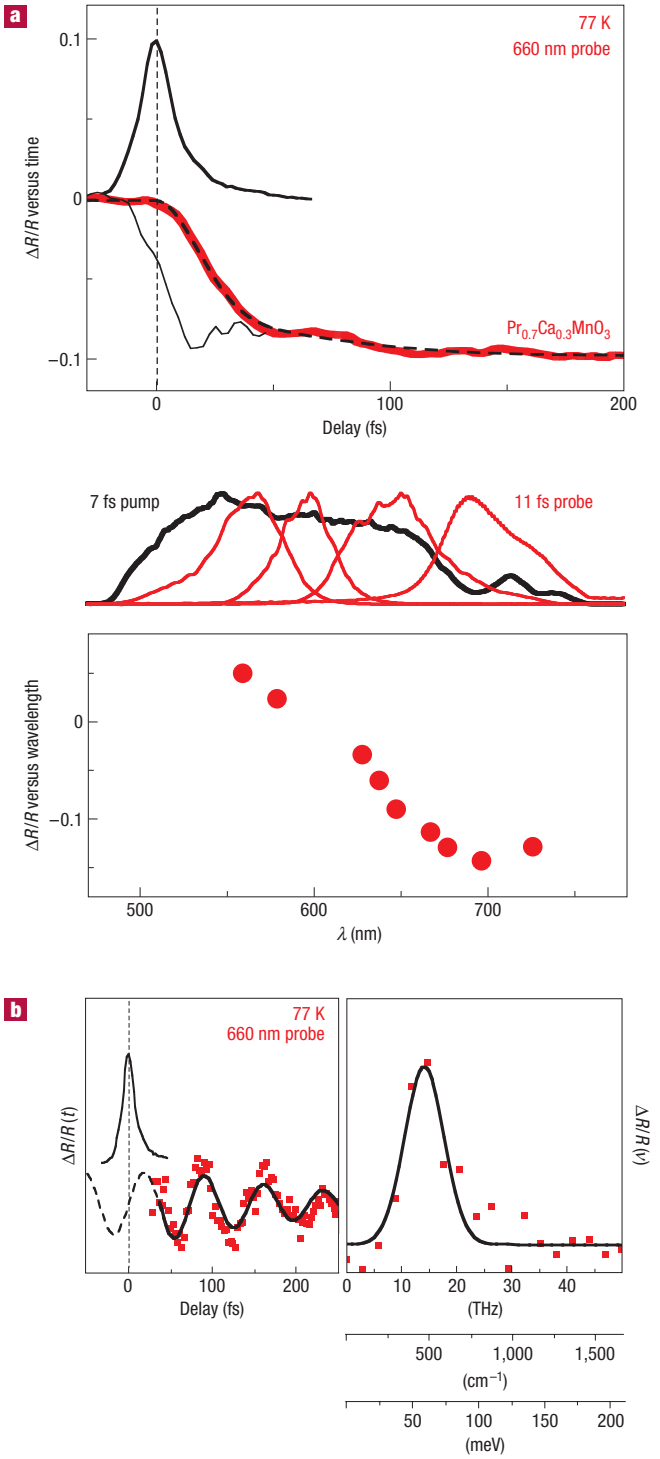

Figure 2 Femtosecond optical reflectivity measurements of $Pr_{0.7}Ca_{0.3}MnO_3$ at 77 K. a, Reflectivity response of $Pr_{0.7}Ca_{0.3}MnO_3$ (red curve), a fit to the delayed reflectivity response (dashed black curve), a pump–probe cross-correlation (thicker black curve), photo-induced transmission changes in a thin film of C_{60} molecules (thinner black curve). The differential reflectivity for different probing wavelengths at a time delay of 500 fs is shown in the lower panel. **b**, Oscillatory time profile obtained by subtracting a fitted biexponential rise from the measured reflectivity transient. The phase of the oscillation is zero at the instant of photo-excitation, indicative of ISRS excitation. The amplitude Fourier transform of this over-damped mode is also shown in the right panel, showing broadband excitation of many modes at once.

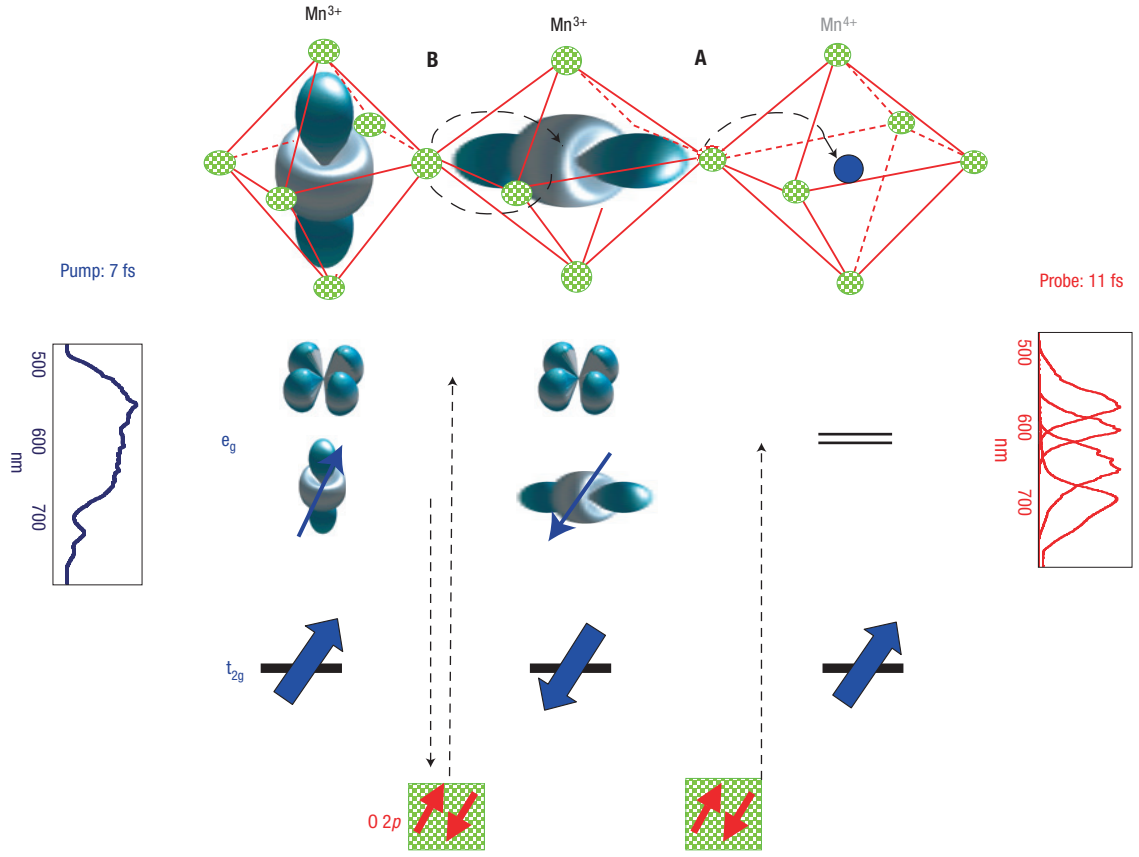

Figure 3 Excitation process in $Pr_{0.7}Ca_{0.3}MnO_3$ in the 2.5 eV photon-energy range. 7 fs optical pulses excite transitions between the O 2*p* states and a coherent superposition of both Jahn–Teller split e_g states of the $Mn^{3+/4+}$ sites. Both direct photo-doping (mechanism A) and ISRS (mechanism B) correspond to the creation of charge and orbital defects. As discussed in the text, analysis of the temporal phase of the oscillatory signal indicates that mechanism B is dominant. On the left-hand side of the diagram, we plot the measured spectrum of the pump pulse, covering a bandwidth of more than 200 nm. On the right-hand side, we show the corresponding spectra of probing pulses of slightly longer duration, used to measure the response of the system at different wavelengths.

Figure 3 shows the possible photo-excitation mechanisms for the coherent vibrations. One mechanism corresponds to a pure transfer of charge from the O 2*p* states to the $Mn^{3+/4+}$ sites (mechanism A). Such photo-doping, if prompt compared with the period of a Raman-active mode, can result in its displacive excitation in the electronically excited state[23]. Displacive excitation of coherent phonons is related to the imaginary part of the Raman tensor, corresponds to the absorption of light and has a cosine-like temporal response. The second channel is possible only at the Mn^{3+} sites, where photo-excitation populates the upper unoccupied e_g state and depopulates the lower-lying one, leaving a quantum of excitation in the system but maintaining charge neutrality (mechanism B). In this case, a vibration is excited impulsively in the electronic ground state[24,25]. This process is referred to as impulsive stimulated Raman scattering (ISRS), is related to the real part of the Raman tensor and has a sine-like temporal response. The vibrational oscillations of Fig. 2a behave like a sine wave, exhibiting zero phase at the instant of photo-excitation and clarifying that the latter mechanism, ISRS, triggers the observed dynamics.

Summarizing our observations for the low-temperature charge-ordered phase: coherent lattice vibrations associated with the motion of the oxygen atoms are excited by ISRS. These displacements couple to the Jahn–Teller distortion, and possibly also to the Mn–O–Mn angle (tolerance factor), mediating melting of charge order. This observation is consistent with our understanding of manganites below the charge ordering temperature, T_{co}. Because a Jahn–Teller distortion and a non-cubic perovskite structure stabilize the parent insulating phase, ultrafast melting of charge and orbital order is probably associated with the motion of the oxygen atoms.

We now turn to the most provocative observation of our paper, that involving the dynamics of the phase change when initiated in the room-temperature phase. Above $T_{co} = 220$ K, $Pr_{0.7}Ca_{0.3}MnO_3$ behaves as a small-polaron insulator with no long-range Jahn–Teller distortion[26]. In this phase, no colossal negative magnetoresistive behaviour is observed. However, with photo-excitation we still observed the formation of a metallic state for approximately the same excitation fluence as that found at low temperatures (see Fig. 4a). The spectral dependence of the differential reflectivity is qualitatively similar to that shown in Fig. 2a, although the zero crossing occurs at longer wavelength, owing to a shift in the charge-transfer transition energy. The response at 660 nm wavelength then has similar size as that at low temperature but opposite sign. The observation of a photo-initiated metallic phase is quite remarkable, and it is indicative of the existence of a competing conducting phase all the way to room temperature. Presumably, colossal negative magnetoresistance does not occur because of the low energy scale of magnetic fields, whereas the 'barrier' between the two phases can be overcome with photo-excitation.

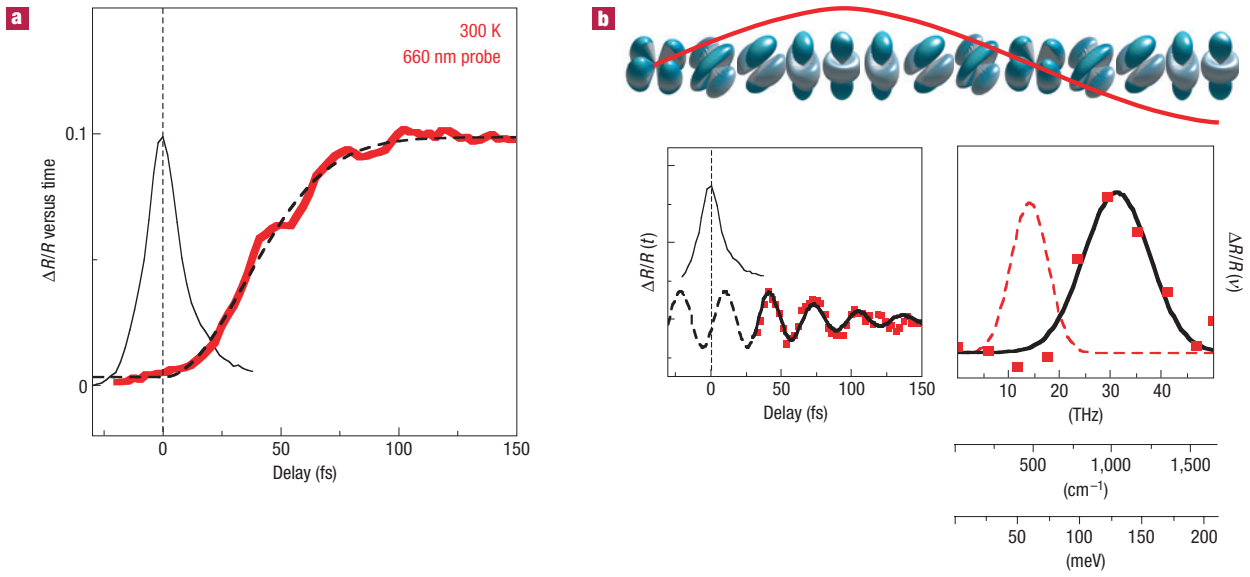

Figure 4 Femtosecond optical reflectivity measurements of $Pr_{0.7}Ca_{0.3}MnO_3$ at 300 K. a, Heavily damped excitations near 31 THz accompany the phase transition. **b**, Oscillations at a frequency that is well beyond that of vibrational excitations (dashed curve) are observed. The sine-like phase of the oscillation clarifies the ISRS excitation mechanism, amounting to a simple 'flipping' of a pseudospin. Above the graph, a pictorial representation of a time-dependent orbital wave on a single site is shown.

Significantly, the coherent excitations that accompany charge delocalization are near 31 THz, a frequency too high to be associated with lattice distortions in this crystal structure. Rather, this frequency is commensurate with the energy scale of d–d crystal-field excitations, or orbital waves (31 THz: 135 meV). ISRS of coherent orbital waves, again indicated by sine-like oscillations, is then qualitatively analogous to the excitation of spin waves in ferromagnetic or antiferromagnetic systems, where a spin defect is introduced and a precessional wave is launched. In the present case, the collective orbital excitation probably corresponds to the excitation of a single pseudospin on a Mn^{3+} $3d$ site, effectively 'flipping' one orbital and launching a 'hybridization' wave (see Fig. 4b). Whereas these excitations, or orbital defects, are likely to initially extend only over the coherence length of small polarons, an 'orbital wave' may propagate beyond this length and accompany the coalescence of different clusters into the metallic phase.

Evidence for orbital modes close to equilibrium has been claimed from Raman experiments in a different perovskite manganite[27] and in titanates[28], where energy shifts corresponding to the frequencies measured here were detected. Yet, a competing interpretation of the manganite experiments has argued that such peaks may have instead arisen from multi-phonon excitation[29]. It is important to stress that the conditions of our experiments are far from equilibrium, and the heavily photo-excited state ($\sim 10^{22}$ absorbed photons cm^{-3}) could well be characterized by a different spectrum of excitations than those probed in Raman scattering. Thus, a direct comparison cannot be made.

However, the possibility of multiple-phonon excitation should be discussed also for our experiments. The theory supporting the existence of large-amplitude multiple-phonon excitations in Raman experiments addresses this issue in terms of a self-trapping exciton in the Franck–Condon state of a localized MnO_6 'molecule'. For the Raman experiments, emission of inelastically scattered radiation is then coupled to a multiply excited ground-state vibration, corresponding to multiple-phonon peaks[30]. However, our experiments can easily discriminate between these two possibilities, at least in a localized picture. In fact, unlike in Raman experiments where the energy of an excitation is measured, we directly detect its frequency, ν. Thus, we can discriminate between a multiply excited oscillator (which still exhibits the fundamental frequency ν_1, increased amplitude and where $E_{\mathrm{Raman}} = 2h \cdot \nu_1$) and a singly excited one with higher energy (where the frequency ν_2 is high and where $E_{\mathrm{Raman}} = h \cdot \nu_2$). Thus, we can safely exclude the possibility of a two-phonon response triggered by self-trapping of a localized exciton.

The other possibility would be the excitation of a true two-phonon state of an extended solid, sometimes referred to as vacuum squeezing of phonon fields[31]. The time-domain oscillations then would not correspond to atomic motions but to oscillations in the variance of the phonon-coordinate expectation value[32]. If this were the case, we should observe both the fundamental frequency and a weaker contribution at the sum frequency, which we do not. This leaves only the possibility of a phonon signal forbidden by symmetry at $k = 0$, where optical probing is carried out. However, if this were the case, a low-frequency phonon contribution should also not be observable in the low-temperature phase, which has the same crystallographic structure as the high-temperature phase. Yet, at low temperatures we see only the low-frequency vibrational excitation. On the basis of these arguments, we conclude that low- and high-frequency oscillations are associated with different modes of the system, namely vibrational and orbital excitations.

In summary, the picture that emerges from probing the photo-induced insulator–metal transition with high temporal resolution is one where collective rearrangements are responsible for a time-delayed charge-delocalization process. Different coherent excitations accompany the phase change. In the low-T phase, where a long-range Jahn–Teller distortion stabilizes the parent insulator, a coherent vibrational mode is observed across the ultrafast 'melting' pathway of charge and orbital order. More provocative are the observations in the small-polaron phase, where no long-range Jahn–Teller distortion is present. In this case, we also find a phase change to a metastable metallic phase, accompanied by a coherent mode at higher frequencies, suggestive of a coherent orbital wave. Much remains to be understood of

the ensuing dynamics, especially how this localized electronic excitation couples to other degrees of freedom, including magnetic excitations. Furthermore, new questions arise on how local photo-domains coalesce into a ferromagnetic metallic phase. In the future, femtosecond X-ray experiments may separately measure dynamics of the lattice[33] and of electronic[34] or magnetic degrees of freedom, extending work carried out in the past on longer timescales and shedding new light onto the non-equilibrium physics of photo-induced phase transitions in complex materials.

MATERIALS AND METHODS

$Pr_{0.7}Ca_{0.3}MnO_3$ single-crystal samples were grown with the floating-zone method, cut and polished to a mirror finish for optical experiments. Laue diffraction was used to check the quality of the single-crystal samples after processing.

Measurements of the time-dependent sample resistivity (see Fig. 1) were carried out as follows. Gold electrodes with a 200-μm-wide gap are deposited on the sample surface, and are d.c.-biased at 30 V. Laser pulses excited the sample with the laser spot fully covering the space between the electrodes. The current flowing through the sample was monitored by measuring the voltage drop across a 50-Ω resistor. The high-conductivity state develops within the 4-ns resolution of the electronics, and exhibits a similar resonance behaviour as observed in the optical measurements.

For the femtosecond pump–probe experiments, independently tunable ultrafast pulses of sub-10-fs duration were derived from two non-collinear optical parametric amplifiers using beta-barium borate crystals. Each optical parametric amplifier was pumped by the second harmonic of Ti:sapphire, seeded by a white-light continuum and compressed by a chirped mirror pair[35].

Received 11 January 2007; accepted 6 July 2007; published 12 August 2007.

References

1. Myiano, K., Tanaka, T., Tomioka, Y. & Tokura, Y. Photo-induced insulator–metal transition in a perovskite manganite. *Phys. Rev. Lett.* **78**, 4257–4260 (1997).
2. Cavalleri, A. *et al.* Femtosecond structural dynamics in VO_2 during a femtosecond solid–solid phase transition? *Phys. Rev. Lett.* **87**, 237401–237404 (2001).
3. Cavalleri, A. *et al.* Anharmonic lattice dynamics in germanium measured with ultrafast X-ray diffraction. *Phys. Rev. Lett.* **85**, 586–589 (2000).
4. Chollet, M. *et al.* Gigantic photoresponse in 1/4-filled-band organic salt $(EDO\text{-}TTF)_2PF_6$. *Science* **307**, 86–89 (2005).
5. Okamoto, H. *et al.* Ultrafast photoinduced melting of a spin-Peierls phase in an organic charge-transfer compound, K-tetracyanoquinodimethane. *Phys. Rev. Lett.* **96**, 037405–037408 (2006).
6. van der Brink, J., Horsch, P., Mack, F. & Oles, A. M. Orbital dynamics in ferromagnetic transition-metal oxides. *Phys. Rev. B* **59**, 6795–6805 (1999).
7. Feiner, L. F. & Oles, A. M. Electronic origin of magnetic and orbital ordering in insulating $LaMnO_3$. *Phys. Rev. B* **59**, 3295–3298 (1999).
8. Dagotto, E. *Nanoscale Phase Separation and Colossal Magnetoresistance* (Springer, Berlin, 2003).
9. Goodenough, J. B. Theory of the role of covalence in the perovskite-type manganites [La, M(II)]MnO_3. *Phys. Rev.* **100**, 564–573 (1955).
10. Zimmermann, M. v. *et al.* Interplay between charge, orbital, and magnetic order in $Pr_{1-x}Ca_xMnO_3$. *Phys. Rev. Lett.* **83**, 4872–4875 (1999).
11. Millis, A. J., Littlewood, P. B. & Shraiman, B. I. Double exchange alone does not explain the resistivity of $La_{1-x}Sr_xMnO_3$. *Phys. Rev. Lett.* **74**, 5144–5147 (1995).
12. Hwang, H. Y., Cheong, S. W., Radaelli, P. G., Marezio, M. & Battlog, B. Lattice effects on the magnetoresistance in doped $LaMnO_3$. *Phys. Rev. Lett.* **75**, 914–917 (1995).
13. Yoshizawa, H., Kawano, H., Tomioka, Y. & Tokura, Y. Neutron-diffraction study of the magnetic-field-induced metal-insulator transition in $Pr_{0.7}Ca_{0.3}MnO_3$. *Phys. Rev. B* **52**, R13145 (1995).
14. Fiebig, M., Miyano, K., Tomioka, Y. & Tokura, Y. Visualization of the local insulator–metal transition in $Pr_{0.7}Ca_{0.3}MnO_3$. *Science* **280**, 1925–1928 (1998).
15. Asamitsu, A., Tomioka, Y., Kuwahara, H. & Yokura, Y. Current switching of resistive states in magnetoresistive manganites. *Nature* **50**, 388–390 (1997).
16. Kiryukhin, V. *et al.* An X-ray-induced insulator–metal transition in a magnetoresistive manganite. *Nature* **386**, 813–815 (1997).
17. Hervieu, M., Barnabé, A., Martin, C., Maignan, A. & Raveau, B. Charge disordering induced by electron irradiation in colossal magnetoresistant manganites. *Phys. Rev. B* **60**, 726–729 (1999).
18. Satoh, K. & Ishihara, S. Photo-induced phase transition in charge ordered perovskite manganites. *J. Magn. Magn. Mater.* **310**, 798–800 (2007).
19. Fiebig, M., Miyano, K., Tomioka, Y. & Tokura, Y. Reflection spectroscopy on the photoinduced local metallic phase of $Pr_{0.7}Ca_{0.3}MnO_3$. *Appl. Phys. Lett.* **74**, 2310–2312 (1998).
20. Okimoto, Y., Tomioka, Y., Onose, Y., Otsuka, Y. & Tokura, Y. Charge ordering and disordering transitions in $Pr_{1-x}Ca_xMnO_3$ ($x = 0.4$) as investigated by optical spectroscopy. *Phys. Rev. B* **57**, 9377–9380 (1998).
21. Cavalleri, A., Dekorsy, Th., Chong, H. H. W., Kieffer, J. C. & Schoenlein, R. W. Evidence for a structurally-driven insulator-to-metal transition in VO_2: A view from the ultrafast timescale. *Phys. Rev. B* **70**, 161102–161106(R) (2004).
22. Yamamoto, K., Kimura, T., Ishikawa, T., Katsufuji, T. & Tokura, Y. Raman spectroscopy of the charge-orbital ordering in layered manganites. *Phys. Rev. B* **61**, 14706–14715 (2001).
23. Garret, G. A., Albrecht, T. F., Whitaker, J. F. & Merlin, R. Coherent THz phonons driven by light pulses and the Sb problem: What is the mechanism? *Phys. Rev Lett.* **77**, 3661–3664 (1996).
24. Dougherty, T. P., Wiederrecht, G. P. & Nelson, K. A. Impulsive stimulated Raman scattering experiments in the polariton regime. *J. Opt. Soc. Am. B* **9**, 2179–2189 (1992).
25. Stevens, T. E., Kuhl, J. & Merlin, R. Coherent phonon generation and the two stimulated Raman tensors. *Phys. Rev. B* **65**, 144304–144307 (2002).
26. Nelson, C. S. *et al.* Correlated polarons in dissimilar perovskite manganites. *Phys. Rev. B* **64**, 174405–174410 (2001).
27. Saitoh, E. *et al.* Observation of orbital waves as elementary excitations in a solid. *Nature* **410**, 180–182 (2001).
28. Ulrich, C. *et al.* Raman scattering in the Mott insulators $LaTiO_3$ and $YTiO_3$: Evidence for orbital excitations. *Phys. Rev. Lett.* **97**, 157401–157403 (2006).
29. Grüninger, M. *et al.* Orbital physics (communication arising): Experimental quest for orbital waves. *Nature* **418**, 39 (2002).
30. Allen, P. B. & Prebeinov, V. Multiphonon resonant Raman scattering predicted in $LaMnO_3$ from the Franck–Condon process via self-trapped excitons. *Phys. Rev. B* **64**, 085118–085123 (1999).
31. Garret, G. A., Rojo, A. G., Sood, A. K., Whitaker, J. F. & Merlin, R. Vacuum squeezing of solids: Macroscopic quantum states driven by light pulses. *Science* **275**, 1638–1640 (1997).
32. Bartels, A., Dekorsy, Th. & Kurz, H. Impulsive excitation of phonon-pair combination states by second-order Raman scattering. *Phys. Rev. Lett.* **84**, 2981–2984 (2000).
33. Cavalleri, A. *et al.* Tracking the motion of charges in a terahertz light field by femtosecond X-ray diffraction. *Nature* **442**, 644–646 (2006).
34. Cavalleri, A. *et al.* Band-selective measurements of electron dynamics in VO_2 using femtosecond near-edge X-ray absorption. *Phys. Rev. Lett.* **95**, 67405–67408 (2005).
35. Manzoni, C., Polli, D. & Cerullo, G. Two-color pump–probe system broadly tunable over the visible and the near infrared with sub-30 fs temporal resolution. *Rev. Sci. Instrum.* **77**, 023103 (2006).

Acknowledgements

The authors are grateful to the following colleagues for discussions: P. B. Allen, E. Dagotto, M. Grueninger, A. T. Boothroyd. Work at the University of Oxford was supported by the European Science Foundation through a European Young Investigator Award, and by Oxford University Press through a John Fell Award. S.W. and A.C. acknowledge support from the European Community Access to research infrastructure action of the Improving Human Potential Programme (LASERLAB Europe). Work at Lawrence Berkeley National Laboratory was supported by the Director, Office of Science, Office of Basic Energy Sciences, Materials Sciences and Engineering Division, of the US Department of Energy.
Correspondence and requests for materials should be addressed to A.C.

Competing financial interests

The authors declare no competing financial interests.